Construction of a 4 Zeptoliters Switchable 3D DNA Box Origami

Reza M. Zadegan,[†,‡,§] Mette D. E. Jepsen,[†,‡,§] Karen E. Thomsen,[§] Anders H. Okholm,[†,‡,§] David H. Schaffert,[†,‡,§] Ebbe S. Andersen,[†,‡,§] Victoria Birkedal,[‡,§] and Jørgen Kjems[†,‡,§,*]

[†]Department of Molecular Biology and Genetics, [‡] Danish National Research Foundation: Centre for DNA Nanotechnology (CDNA) and [§] Interdisciplinary Nanoscience Center (iNANO), Aarhus University, DK-8000 Aarhus, Denmark

ABSTRACT The DNA origami technique is a recently developed self-assembly method that allows construction of 3D objects at the nanoscale for various applications. In the current study we report the production of a 18 × 18 × 24 nm^3 hollow DNA box origami structure with a switchable lid. The structure was efficiently produced and characterized by atomic force microscopy, transmission electron microscopy, and Förster resonance energy transfer spectroscopy. The DNA box has a unique reclosing mechanism, which enables it to repeatedly open and close in response to a unique set of DNA keys. This DNA device can potentially be used for a broad range of applications such as controlling the function of single molecules, controlled drug delivery, and molecular computing.

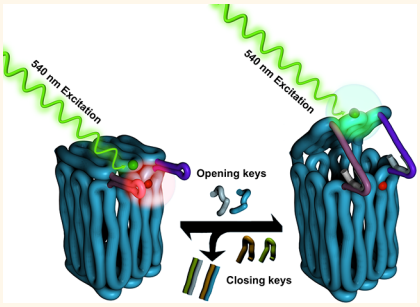

KEYWORDS: 3D DNA origami · dynamic origami · multiswitchable nanostructure · FRET

DNA origami was originally developed to create 2D nanoscale DNA structures[1−3] and subsequently used to create defined and more sophisticated 3D nanoscale architectonics,[4−8] some of which are functionalized for specific applications.[9−21] Owing to their phenomenal addressability, multifunctional 3D DNA nanostructures can readily be designed for a particular purpose.[22] For instance, hollow structures with addressable surfaces are desirable for designing drug delivery containers and we have previously constructed a 42 × 36 × 36 nm^3 DNA box using a full-length single stranded (ss) M13 DNA scaffold.[5]

Smaller 3D DNA nanostructures have been reported; from tile-based structures such as tetrahedron,[23,24] prisms,[25] octahedron,[24] dodecahedron, and bucky balls[24] to the more complex origami like structures such as octahedron,[26] and small solid 3D DNA structures.[4] However, none of these structures combine closed surfaces with a hollow cavity with the potential capacity to accommodate cargo. Also, the opening mechanism of the previously reported 3D origami structure was an irreversible process, incapable of multiple switching events.

To address these issues we designed a smaller reconfigurable DNA box with estimated total external and internal cavity dimensions of 18 × 18 × 24 and 14 × 14 × 20 nm^3, respectively, which corresponds approximately to $^1/_7$ of the volume of our previously reported DNA box[5] (Figure 1b and Supporting Information section S1). The self-assembled structure encompasses a 1983 nucleotides single-stranded DNA, derived from a truncated pUC plasmid, and 59 short single-stranded staple DNA oligos, that together form a 110k atoms complex with a molecular weight of 1.3 MDa. Moreover, the small 3D DNA box origami is multiswitchable and capable of undergoing multiple rounds of openings and closures in response to externally provided keys.

RESULTS AND DISCUSSION

The DNA box was assembled in a single-step annealing process and characterized by gel analysis, dynamic light scattering (DLS), atomic force microscopy (AFM), and transmission electron microscopy (TEM) which all indicated an efficient assembly process (Figure 1 and Supporting Information sections S4, S5, S6, and S7). The assembly yield was estimated to be approximately 90% (Supporting Information Figure S6-2). The assembled DNA box origamies appeared as empty "frames" (Figure 1a), which can be explained by higher density of the projected stained DNA helices of boxes lying on the side. The preference for this position probably reflects the increased surface interaction between negatively charged DNA with the positively charged surface. Misfolded structures were rarely observed

* Address correspondence to jk@mb.au.dk.

Received for review August 17, 2012 and accepted October 2, 2012.

Published online October 02, 2012
10.1021/nn303767b

© 2012 American Chemical Society

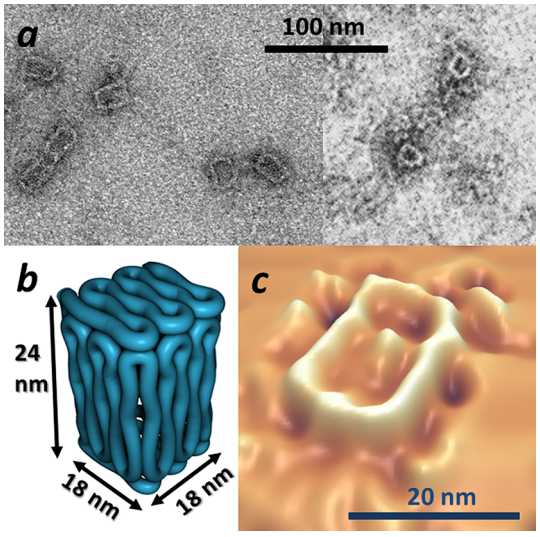

Figure 1. TEM image of the DNA box origami. (a) Zoom-out micrograph showing examples of DNA box origami particles. The left panel illustrates the particles which lie on the long sides of the structure. The right panel represents some particles which lie on the lid or bottom of the box. (b) Graphical model of the structure. (c) Image processed demonstration of a randomly selected particle where the area was sharpened and averaged to gain a better perception of the DNA box frame. This image does not show the height (3rd dimension) of the structure, and the projected areas of the frame are calculated based on the signal intensity of the particle frame from the 2D TEM image.

indicative of a very high assembly yield. The dimensions of the structure are slightly (0−5 nm) smaller than the predicted size (Figure 1b) which may be caused by the negative stain procedure used for TEM imaging, as reported previously.[27] For better visualization, randomly selected areas of the TEM images were further image processed (Figure 1c).

To control the opening of the box, two locks were designed and inserted between the lid and the side (Supporting Information section S1). Each lock contains a unique 8-nucleotide toehold which, upon addition of the right keys (composed of ss-DNA strands with sequences corresponding to two breast cancer specific microRNA 223[28] and microRNA 30c[29]), causes the displacement of the two locks and leads to the opening of the DNA box lid (Figure 2a). To examine the opening process, we performed Förster resonance energy transfer (FRET) spectroscopy measurements. A FRET pair (Cy3 and Cy5 dyes) was attached to two different oligos placed at an estimated distance of approximately 3 nm from each other in the closed state. Upon opening of the lid the distance between the dyes is expected to increase and thus causes the FRET efficiency to decrease.

Figure 2b shows typical fluorescence spectra after donor excitation for a closed box (blue curve) and after lid opening (red curve). Donor fluorescence intensity peak is at ∼560 nm and the appearance of acceptor fluorescence peak at 670 nm indicates the presence of energy transfer between the two dyes in the closed state. Upon key addition, acceptor fluorescence disappears almost completely and the intensity of donor fluorescence increases significantly, implying a decrease in the energy transfer due to an increased separation of the two dyes. The FRET efficiencies are ∼0.9 and ∼0.1 in the closed and open states, respectively, consistent with efficient opening of the DNA box origami (Figure 2c).

As previously observed for the larger DNA box with a similar key design,[5] closing the lid by removing the key is not efficient (Supporting Information, Figure S9). Therefore, we designed another lock-and-key system, which more efficiently reconfigures the box to a closed state (Supporting Information, Figure S1-9). In this system the first pair of opening keys ($K1_O$ and $K2_O$) bind to the two toeholds in the loops, respectively, and by strand displacement unzip the two locks. To enable the removal of the keys an overhang of eight bases was introduced at the 5′-end of the opening keys which, can hybridize to the pair of closing keys ($K1_C$ and $K2_C$), causing displacement of the opening keys from the locks and closure of the lid. The cycle was repeated in the same reaction mixture by adding of opening and closing keys in alternating cycles (at concentration denoted in Figure 2e). The opening and closure cycles of the DNA box structures were studied using a box with either two different or identical lock sequences (setup 1 and setup 2, respectively). We successfully opened and reclosed the box structure for three rounds for both setups demonstrating the robustness of the system (Figure 2e).

CONCLUSION

In summary, we demonstrated the assembly of the so far smallest hollow and reconfigurable 3D DNA box origami nanostructure capable of going through at least three efficient opening and closing events. The DNA box origami design presented here has valuable potential applications. The small size may ease the self-assembly process, indicated by the very high yield of well-formed boxes, and may also increase stiffness and robustness, without jeopardizing the unique addressability and reproducibility of origami structures. It may also facilitate translocation through biological barriers including cell membranes but remains large enough to host macromolecules like enzymes and antibodies. The programmability of the lid can be used to control delivery or accessibility of cargo on demand, or control chemical and enzymatic reactions by precluding two components from one another in a controlled fashion. Importantly, our DNA box has an asymmetric structure that leaves out the inevitable seams of symmetric structures, and thus theoretically results in smaller holes in the box surfaces and reduced leakage as compared to the symmetric structures. The next challenge is to deliver the small box DNA origami into the cells

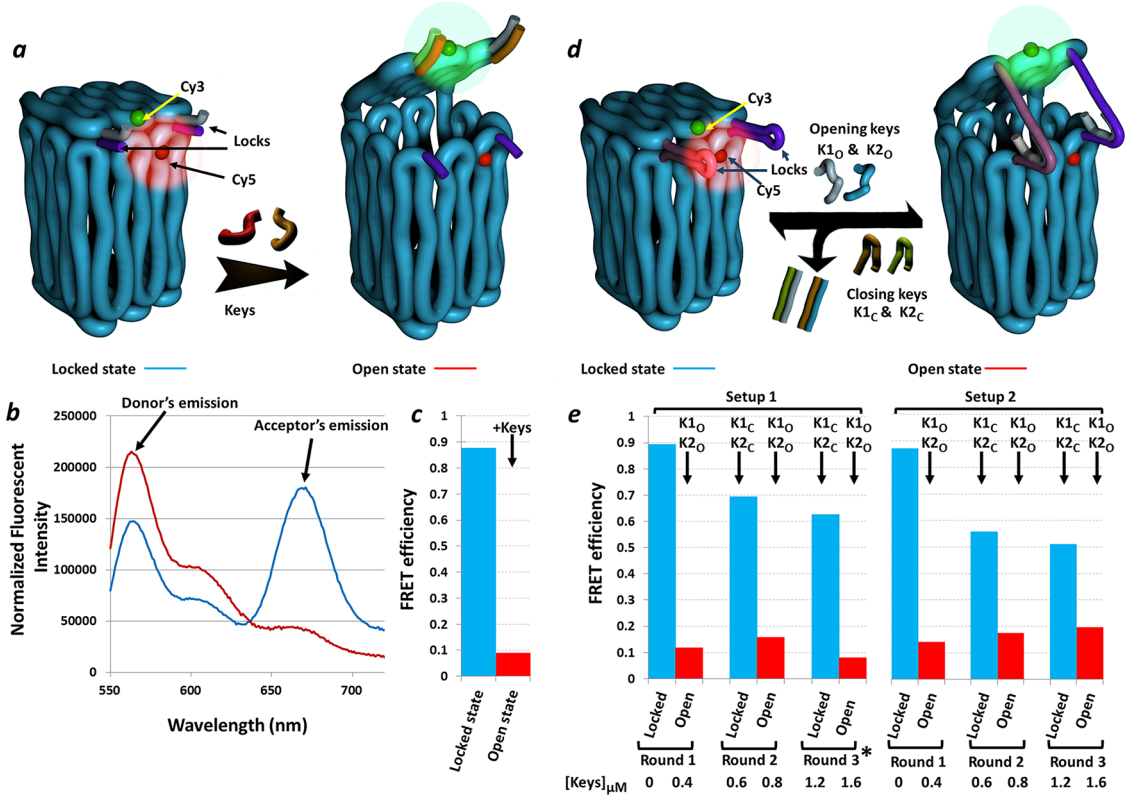

Figure 2. FRET studies of opening/closing of the small DNA box origami. (a) Schematic illustration of the lid opening process. The addition of matching keys unzips the locks and the lid opens presumably due to electrostatic repulsion of negative charge of the DNA. (b) Fluorescence spectra of box samples in the closed (blue line) and open (red line) states. (c) Blue and red columns indicate the FRET efficiencies in closed and open states of the box, respectively. (d) Schematic illustration of DNA box origami with multiswitchable lock system. Upon addition of the opening keys ($K1_O$ and $K2_O$) the structure will be opened and the FRET efficiency decreases, whereas addition of closing keys ($K1_C$ and $K2_C$) in 1.5 molar excess closes the lid and restores efficient FRET. (e) Quantification of FRET values through three cycles of opening and closing using increasing concentrations of opening and closing keys as indicated below the chart. Setups 1 and 2 refer to experimental conditions where either two different or identical keys are applied to two matching locks, respectively. During the last round of sample Setup 1 (indicated with star), the fluorescence peak of Cy3 was observed to shift to higher energy by a few nanometers, which indicates that there may be a change in the environment of the fluorophore.

and study its response to intracellular cues. The present box has been designed to respond to miR223 and miR30c, which are signatures of breast cancer cells. It is conceivable that we in the future can use our DNA origami devices to deliver drugs only to cancer cells that express a particular set of miRNAs. This will create an additional level of specificity and potentially decrease off-target effects.

MATERIALS AND METHODS

Scaffold Strand Production. A 1983 bases long single-stranded DNA template was produced. pUC118 plasmid (Clontech) containing M13 origin of replication was reduced in size in a three-steps process. The produced plasmid (pUC1983) was transformed into XL1-Blue Supercompetent Cells (Stratagen). The production of single stranded pUC1983 (ss-pUC1983) was induced upon transfection of the cells with M13KO7 helper phage (New England Biolabs).

DNA Origami Assembly and Purification. A 5 nM solution of DNA origami in a final concentration of 1× TAE−Mg^{2+} buffer (40 mM Tris pH: 8.0, 2 mM EDTA pH: 8.0, 12.5 mM $MgAc_2$) was produced in a 60 h annealing process. The assembled structures were purified using Illustra MicroSpin S-400 HR Columns (GE Healthcare Life Sciences).

TEM Analysis. Five femtomole of purified DNA origami solution was loaded on a glow discharged, 300 mesh carbon-coated nickel grid and stained with 1% uranyl acetate for 1 min. TEM imaging was operated by FEI CM100 microscope at 80 kV, with a MegaView III camera or a FEI Tecnai12 microscope at 120 kV with a Gatan 1 × 1 camera. The single particles were selected using the Boxer program of the EMAN2 package.[30] Projected presentations of the selected particles were produced using FemtoScan (Advanced Technologies Center) through several rounds of Median and Winer filtering of selected areas with arbitrary masks. Finally those selected areas were sharpened and averaged with a mask of arbitrary width to render the final images.

Opening of the Closed DNA Box Origami. Opening of the closed DNA origami was induced using a pair of proper keys (in 10 times molar excess) and the FRET measurements of the open state DNA box origami was conducted at 25 °C immediately after the addition of the keys.

Opening and Closing of the DNA Box Origami. Opening and reclosing of the box were performed by the addition (in 50% molar excess) of opening ($K1_O$ and $K2_O$) and reclosing ($K1_C$ and $K2_C$) keys, respectively. The time intervals after addition of the

opening and closing keys were set to 15 and 60 min, respectively. The same settings have been used for both setup 1 and setup 2 systems.

FRET Measurements. Steady-state fluorescence measurements were performed on a Fluoromax 3 fluorometer [Horiba Jobin-Yvon] at 25 °C and with a sample volume of 65 μL. Fluorescence was excited at 530 nm (excitation of Cy3) and 600 nm (excitation of Cy5), the entrance and exit slits were set to 10 nm, and integration time was set to 0.5 s. FRET efficiencies were calculated using the ratio A method[31] as $E = \varepsilon_{DA}(I_{AD}/I_{AA} - \varepsilon_{AA})$, where I_{AD} is the acceptor peak fluorescence intensity after donor excitation from which contribution from donor fluorescence was subtracted, I_{AA} is the acceptor peak fluorescence intensity after acceptor excitation, and the values for ε_{AA} and ε_{DA} were determined from absorption spectra as 0.07 and 1.03, respectively.

Conflict of Interest: The authors declare no competing financial interest.

Supporting Information Available: Extended materials and methods including designs, further gel, AFM and TEM images, FRET and DLS studies, computer codes, and list of sequences. This material is available free of charge *via* the Internet at http://pubs.acs.org.

Acknowledgment. This work was supported by grants from the Danish National Research Foundation to the CDNA Center, from the Danish Council for Independent Research's carrier program Sapere Aude, from the Lundbeck foundation and by Aarhus University. The authors would like to thank professor Kurt V. Gothelf, Rita Rosendahl, and Rasmus S. Sørensen for their helpful contributions to this project.

REFERENCES AND NOTES

1. Rothemund, P. W. Folding DNA to Create Nanoscale Shapes and Patterns. *Nature* **2006**, *440*, 297–302.
2. Qian, L.; Wang, Y.; Zhang, Z.; Zhao, J.; Pan, D.; Zhang, Y.; Liu, Q.; Fan, C.; Hu, J.; He, L. Analogic China Map Constructed by DNA. *Chin. Sci. Bull.* **2006**, *51*, 2973–2976.
3. Endo, M.; Sugita, T.; Rajendran, A.; Katsuda, Y.; Emura, T.; Hidaka, K.; Sugiyama, H. Two-Dimensional DNA Origami Assemblies Using a Four-Way Connector. *Chem. Commun.* **2011**, *47*, 3213–3215.
4. Douglas, S. M.; Dietz, H.; Liedl, T.; Hogberg, B.; Graf, F.; Shih, W. M. Self-Assembly of DNA into Nanoscale Three-Dimensional Shapes. *Nature* **2009**, *459*, 414–418.
5. Andersen, E. S.; Dong, M.; Nielsen, M. M.; Jahn, K.; Subramani, R.; Mamdouh, W.; Golas, M. M.; Sander, B.; Stark, H.; Oliveira, C. L. P.; *et al.* Self-assembly of a Nanoscale DNA Box with a Controllable Lid. *Nature* **2009**, *459*, 73–76.
6. Ke, Y.; Sharma, J.; Liu, M.; Jahn, K.; Liu, Y.; Yan, H. Scaffolded DNA Origami of a DNA Tetrahedron Molecular Container. *Nano Lett.* **2009**, *9*, 2445–2447.
7. Dietz, H.; Douglas, S. M.; Shih, W. M. Folding DNA into Twisted and Curved Nanoscale Shapes. *Science* **2009**, *325*, 725–730.
8. Han, D.; Pal, S.; Liu, Y.; Yan, H. Folding and Cutting DNA into Reconfigurable Topological Nanostructures. *Nat. Nanotechnol* **2010**, *5*, 712–717.
9. Stephanopoulos, N.; Liu, M.; Tong, G. J.; Li, Z.; Liu, Y.; Yan, H.; Francis, M. B. Immobilization and One-Dimensional Arrangement of Virus Capsids with Nanoscale Precision Using DNA Origami. *Nano Lett.* **2010**, *10*, 2714–2720.
10. Rinker, S.; Ke, Y.; Liu, Y.; Chhabra, R.; Yan, H. Self-Assembled DNA Nanostructures for Distance-Dependent Multivalent Ligand-Protein Binding. *Nat. Nanotechnol.* **2008**, *3*, 418–422.
11. Stearns, L. A.; Chhabra, R.; Sharma, J.; Liu, Y.; Petuskey, W. T.; Yan, H.; Chaput, J. C. Template-Directed Nucleation and Growth of Inorganic Nanoparticles on DNA Scaffolds. *Angew. Chem., Int. Ed.* **2009**, *48*, 8494–8496.
12. Steinhauer, C.; Jungmann, R.; Sobey, T. L.; Simmel, F. C.; Tinnefeld, P. DNA Origami as a Nanoscopic Ruler for Super-Resolution Microscopy. *Angew. Chem., Int. Ed.* **2009**, *48*, 8870–8873.
13. Ding, B.; Wu, H.; Xu, W.; Zhao, Z.; Liu, Y.; Yu, H.; Yan, H. Interconnecting Gold Islands with DNA Origami Nanotubes. *Nano Lett.* **2010**, *10*, 5065–5069.
14. Liu, J.; Geng, Y.; Pound, E.; Gyawali, S.; Ashton, J. R.; Hickey, J.; Woolley, A. T.; Harb, J. N. Metallization of Branched DNA Origami for Nanoelectronic Circuit Fabrication. *ACS Nano* **2011**, *5*, 2240–2247.
15. Maune, H. T.; Han, S.-p.; Barish, R. D.; Bockrath, M.; Goddard, W. A.; Rothemund, P. W. K.; Winfree, E. Self-Assembly of Carbon Nanotubes into Two-Dimensional Geometries using DNA Origami Templates. *Nat. Nanotechnol.* **2010**, *5*, 61–66.
16. Kershner, R. J.; Bozano, L. D.; Micheel, C. M.; Hung, A. M.; Fornof, A. R.; Cha, J. N.; Rettner, C. T.; Bersani, M.; Frommer, J.; Rothemund, P. W. K.; *et al.* Placement and Orientation of Individual DNA Shapes on Lithographically Patterned Surfaces. *Nat. Nanotechnol.* **2009**, *4*, 557–561.
17. Hung, A. M.; Micheel, C. M.; Bozano, L. D.; Osterbur, L. W.; Wallraff, G. M.; Cha, J. N. Large-Area Spatially Ordered Arrays of Gold Nanoparticles Directed by Lithographically Confined DNA Origami. *Nat. Nanotechnol.* **2010**, *5*, 121–126.
18. Kuzyk, A.; Schreiber, R.; Fan, Z.; Pardatscher, G.; Roller, E. M.; Hogele, A.; Simmel, F. C.; Govorov, A. O.; Liedl, T. DNA-Based Self-Assembly of Chiral Plasmonic Nanostructures with Tailored Optical Response. *Nature* **2012**, *483*, 311–314.
19. Kuzyk, A.; Yurke, B.; Toppari, J. J.; Linko, V.; Törmä, P. Dielectrophoretic Trapping of DNA Origami. *Small* **2008**, *4*, 447–450.
20. Lund, K.; Manzo, A. J.; Dabby, N.; Michelotti, N.; Johnson-Buck, A.; Nangreave, J.; Taylor, S.; Pei, R.; Stojanovic, M. N.; Walter, N. G.; *et al.* Molecular Robots Guided by Prescriptive Landscapes. *Nature* **2010**, *465*, 206–210.
21. Gu, H.; Chao, J.; Xiao, S.-J.; Seeman, N. C. A Proximity-Based Programmable DNA Nanoscale Assembly Line. *Nature* **2010**, *465*, 202–205.
22. Zadegan, R. M.; Norton, M. L. Structural DNA Nanotechnology: From Design to Applications. *Int. J. Mol. Sci.* **2012**, *13*, 7149–7162.
23. Goodman, R. P.; Berry, R. M.; Turberfield, A. J. The Single-Step Synthesis of a DNA Tetrahedron. *Chem. Commun.* **2004**, 1372–1373.
24. He, Y.; Su, M.; Fang, P.-a.; Zhang, C.; Ribbe, A. E.; Jiang, W.; Mao, C. On the Chirality of Self-Assembled DNA Octahedra. *Angew. Chem., Int. Ed.* **2010**, *49*, 748–751.
25. Aldaye, F. A.; Sleiman, H. F. Modular Access to Structurally Switchable 3D Discrete DNA Assemblies. *J. Am. Chem. Soc.* **2007**, *129*, 13376–13377.
26. Shih, W. M.; Quispe, J. D.; Joyce, G. F. A 1.7-Kilobase Single-Stranded DNA that Folds into a Nanoscale Octahedron. *Nature* **2004**, *427*, 618–621.
27. Sander, B.; Golas, M. M. Visualization of Bionanostructures Using Transmission Electron Microscopical Techniques. *Microsc. Res. Tech.* **2011**, *74*, 642–663.
28. Laios, A.; O'Toole, S.; Flavin, R.; Martin, C.; Kelly, L.; Ring, M.; Finn, S. P.; Barrett, C.; Loda, M.; Gleeson, N.; *et al.* Potential Role of miR-9 and miR-223 in Recurrent Ovarian Cancer. *Mol. Cancer* **2008**, *7*, 35.
29. Shen, J.; Ambrosone, C. B.; Zhao, H. Novel Genetic Variants in microRNA Genes and Familial Breast Cancer. *Int. J. Cancer* **2009**, *124*, 1178–1182.
30. Tang, G.; Peng, L.; Baldwin, P. R.; Mann, D. S.; Jiang, W.; Rees, I.; Ludtke, S. J. EMAN2: An Extensible Image Processing Suite for Electron Microscopy. *J. Struct. Biol.* **2007**, *157*, 38–46.
31. Clegg, R. M.; Murchie, A. I.; Zechel, A.; Carlberg, C.; Diekmann, S.; Lilley, D. M. Fluorescence Resonance Energy Transfer Analysis of the Structure of the Four-Way DNA Junction. *Biochemistry* **1992**, *31*, 4846–4856.